

Quantitative Image Analysis with Mathematical Morphology

Alessandro Ledda¹, Jan Quintelier², Pieter Samyn², Patrick De Baets² and Wilfried Philips¹

¹TELIN and ²Laboratory Soete, Ghent University
Sint-Pietersnieuwstraat 41, B-9000 Ghent, Belgium
Phone: +32(9)264.89.00 Fax: +32(9)264.42.95
E-mail: ledda@telin.ugent.be

Abstract— This paper deals with the analysis of shape and size of the debris particles obtained from wear experiments on polymers using image processing. Two analysis techniques that are very promising in this respect are the morphological pattern spectrum and the Fourier spectrum. They can be used to extract parameters that relate to particle size and shape. We experimentally compare different choices for these parameters in order to determine the usefulness of the pattern spectrum in the field of material science. The first tests were done on a polymer called “polyimide”. We performed wear experiments with different temperatures, loads and frequencies. In the future we will perform experiments on composite materials.

Keywords— mathematical morphology; sliding bearing materials; pattern spectrum; opening tree; fast Fourier transform

I. INTRODUCTION

Composite materials are useful as friction bearing materials. They are used, e.g. in the motors of many household appliances and for telescopic arms or sluices. We concentrate on dry bearing materials, which are used without lubrication, as used in e.g. machinery for food and pharmaceuticals processing. In comparison with the traditional bearings, the composite bearings have many advantages: low noise, shock proof, simple assembly and disassembly, high maximum rotational frequencies and high life expectation. As such, there is a great interest in experimentally evaluating their friction and wear properties and relating them to external parameters (motor speed, temperature, pressure, ...). A microscopic study of the fibres can help us understand what is happening physically, and allows us to choose the right materials to build bearing constructions. The microscopic images have to be analysed, so image processing is needed for preprocessing and to do the analysis.

A. Tribology

Tribology is the science and technology of interacting surfaces in relative motion and the practices related thereto [1]. Traditional parameters studied in tribological investi-

gations are the normal and the friction forces, which allow us to determine one of the most important physical parameters: the *friction coefficient*. This parameter is important because friction produces heat, and thus the friction coefficient should be minimized. It depends on many parameters such as normal load, speed and temperature.

Another interesting parameter to measure is the *vertical displacement*. This gives an indication of the wear rate, or how fast a material wears under certain conditions.

Nowadays it is not enough to know how fast materials wear, but we want to understand how they wear, what the major processes are, all in order to pick up the better material combination. Lots of different processes contribute to wear. The most important mechanisms are *adhesion*, *abrasion*, *corrosion*, *fretting*, *pitting* and *delamination*.

II. EXPERIMENTAL SETUP

The test samples are installed onto a *pin-on-plate* setup (Plint TE-77) (fig. 1) where a steel pin applies a normal force on the sample while moving forward and backward. This will wear the material.

To visualise the different types of wear, a camera images the surface of the test samples during the wear process. Also, the debris particles resulting from the wear process are collected and photographed. The analysis of the shape and size of these particles in the pictures will hopefully help us with the understanding of the wear process, and with the correlation between all the parameters collected during a test.

Although this paper deals only with the image processing aspects, the experimental setup also collects other information. Different sensors measure features such as normal and frictional forces, vertical displacement of the pin, acceleration, temperature of the pin and the disk surface, and acoustic emission (a non destructive evaluation technique [2]).

For the experiments described in this paper we have used polymers called “polyimide”. The main difference with a composite material is the absence of fibres that strengthen the polymer. Future experiments will be per-

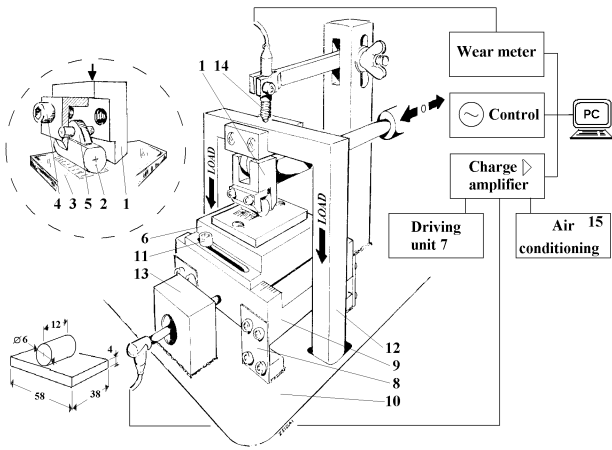


Fig. 1. Experimental setup of the pin-on-plate experiment.

formed on composite sliding materials with a *pin-on-disc* setup. The wear particles look like the ones in fig. 2. The original pictures were colour images with resolution 1300×1030 , but are converted to 8 bit grayscale pictures, since our image processing algorithms only work on monochrome images. For display purposes, we also performed a histogram equalisation to improve the contrast between the background and the particles.

Three parameters are varied in the experiment: *temperature*, *load* and *frequency*.

The friction causes the plate to heat up. The temperature, which started at room temperature, can be regulated to stay at a certain value, or it can be kept free, resulting in further heating up of the plate (“free T” in the table). The load of the pin on the sample varies between 50 N and 200 N. We use different frequencies for the movement speed of the plate.

We have pictures with the following parameter values:

	Temperature (°C)	Load (N)	Frequency (Hz)
1	free T	100	10
2	free T	100	20
3	free T	100	40
4	100	50	10
5	100	100	10
6	100	150	10
7	100	200	10
8	180	50	10
9	180	100	10
10	180	150	10

III. METHODS

Different possibilities are available to extract information from an image. One method is to perform a Fourier transform on the image and to calculate some parameters. Another possibility is to take into account the size and

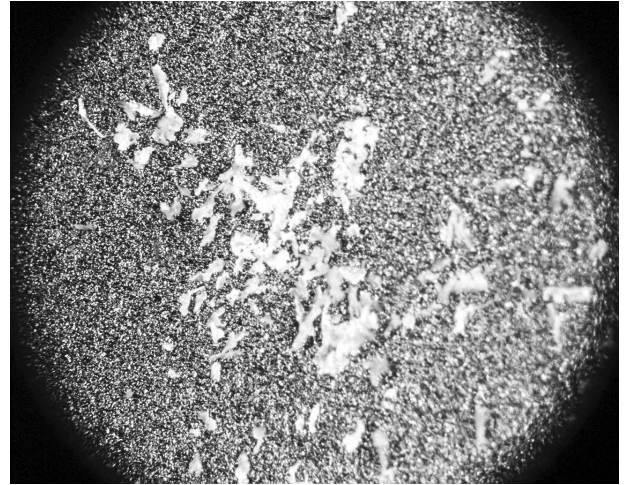


Fig. 2. Grayscale image of the debris particles from a polymer.

shape information of the objects in the image. This can be done with mathematical morphology.

A. Fourier Analysis

The *Fourier transform* [3] of an image gives us an energy spectrum that reflects the grayscale periodicity (spatial frequency spectrum) in the image. Large image objects will have low frequency values, small objects will be represented by the higher frequencies. The Fourier transform lacks the ability of spatial localisation, but in our case this is not a problem, since our debris particles don’t have to be localised. The particles in the pictures don’t behave periodically, but we hope the size distribution has it’s effect on the shape of the Fourier spectrum.

An image is transformed with the two dimensional *Fast (Discrete) Fourier Transform* (FFT). This results in a two dimensional (real) spatial frequency energy spectrum (fig. 3). In order to calculate some first-order histogram features and to remove the orientation dependence of the FFT-spectrum, we transform the 2D-spectrum into a 1D-spectrum (FFTh) with on the abscissa the spatial frequency $\sqrt{\nu_x^2 + \nu_y^2}$. We use Matlab™ for the calculation of the FFTh.

From the histogram, we compute the following parameters, which will be discussed further on:

- *Mean*: the average value:

$$S_M = \bar{b} = \sum_b bP(b), \quad (1)$$

with b the histogram index and $P(b)$ the value of histogram index b divided by the image area;

- *Standard deviation*: the spread of the values:

$$S_D = \sigma_b = \left[\sum_b (b - \bar{b})^2 P(b) \right]^{1/2}; \quad (2)$$

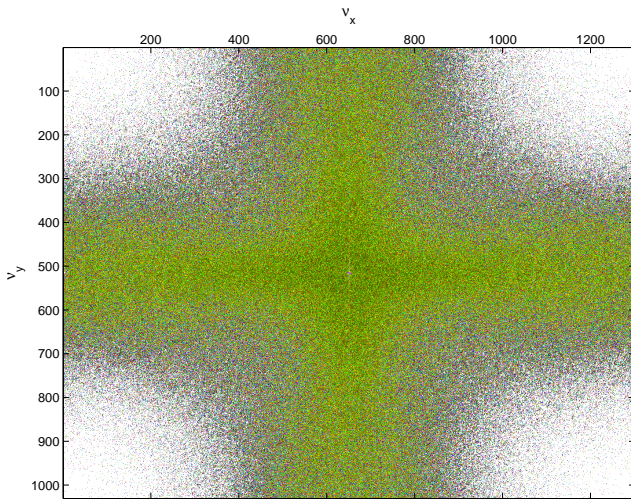


Fig. 3. Fast Fourier Transformed image.

- *Skewness*: the asymmetry of the histogram curve:

$$S_S = \frac{1}{\sigma_b^3} \sum_b (b - \bar{b})^3 P(b); \quad (3)$$

- *Kurtosis*: curve shape relative to a normal distribution:

$$S_K = \frac{1}{\sigma_b^4} \sum_b (b - \bar{b})^4 P(b) - 3; \quad (4)$$

- *Energy*:

$$S_N = \sum_b P(b)^2; \quad (5)$$

- *Entropy*:

$$S_E = - \sum_b P(b) \log_2 P(b). \quad (6)$$

B. Mathematical morphology

Mathematical morphology (MM) [4] is based on set theory. The shapes of objects in a binary image are represented by object membership sets. This theory can be extended to grayscale images. Morphological operations can simplify image data, preserving the objects' essential shape characteristics, and can eliminate irrelevant objects. The main advantage of a morphological filter for example is the ability to preserve the shape of large enough objects, unlike a Gaussian filter which blurs small and big objects indiscriminately. MM is also a useful tool for segmenting regions of interest.

Mathematical morphology is based on two basic operations: *dilation*, which fills holes and smoothens the contour lines, and *erosion*, which removes small objects and disconnects objects connected by a small bridge. Such operations are defined in terms of a *structuring element* (short: *strel*), a small window that scans the image and

alters the pixels in function of its window content. The choice of the proper strel is important. A dilation of image A with strel B ($A \oplus B$) blows up the object, an erosion ($A \ominus B$) lets it shrink (see fig. 4).

Other operations, like the *opening* (an erosion followed by a dilation) and the *closing* (a dilation followed by an erosion), are derived from the basic operators.

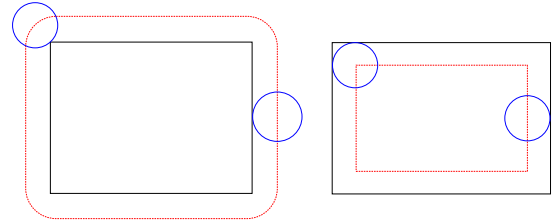


Fig. 4. Schematic example of the basic morphological operators. Solid line: original object; Dashed line: result object; Circle: structuring element. Left: *dilation*; Right: *erosion*.

B.1 Pattern spectrum

If we take a strel and perform an opening on an image, some elements will disappear. If we take a bigger strel, then more elements in the image will vanish. In this way we can determine how the number of eliminated pixels increases when the image is morphologically opened using strels $nB = B \oplus B \oplus \dots \oplus B$ (n times) of increasing size n . The resulting plot of the number of eliminated pixels versus the strel size n is called the *pattern spectrum* (PS) or the *granulometric curve* [5].

The pattern spectrum is a histogram of the distribution of the sizes of various objects displayed in an image. Formally, it is defined as follows:

$$PS(A; B)(n) = \# [A \circ nB \setminus A \circ (n+1)B], n \geq 0 \quad (7)$$

where \circ is the opening symbol, \setminus is the pixelwise difference and $\#$ is the count of grayscale pixels. Note that $0B = \{0\}$.

There is an analogy with the Fourier spectrum: the low frequencies in the Fourier spectrum relate to the global features of the image or the smooth objects, the high frequencies to the details or the fast grayscale variations. Similarly, big structuring elements in the pattern spectrum show the global features of the image or the large smooth objects, while small sized strels also preserve the details or the small rough objects.

An example: fig. 5 shows the pattern spectrum of the first image in the series of fig. 6. In this figure you can see the residues after an opening operation (left to right, top to bottom). First the small objects are eliminated, finally the big ones.

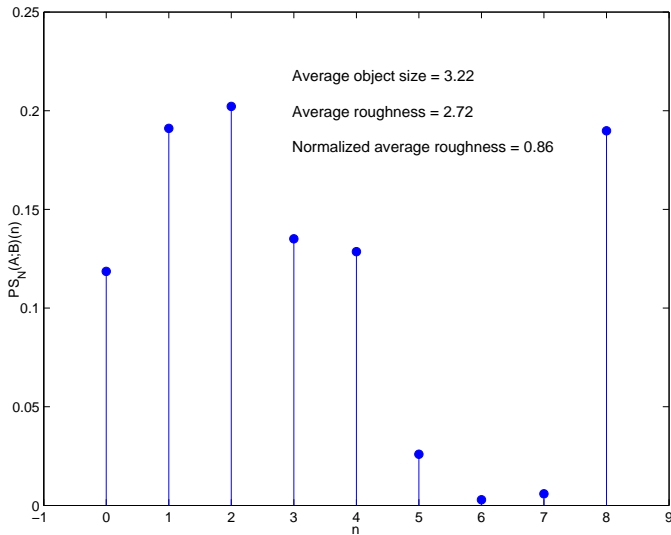


Fig. 5. The pattern spectrum (norm.) of image A (fig. 6 upper left) with opening with structuring element B (a disk with radius 5).

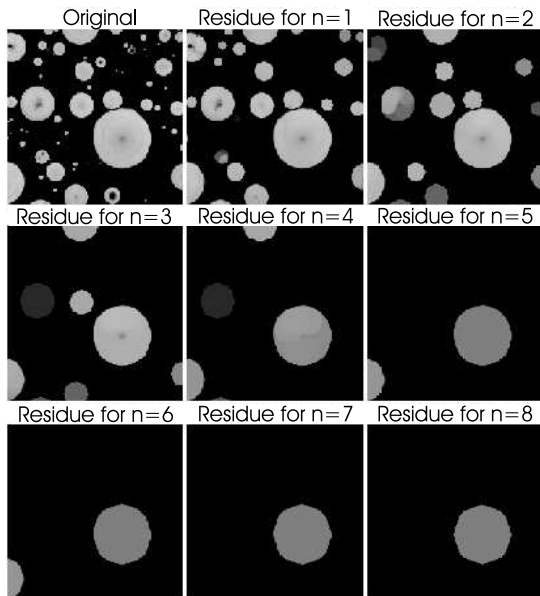


Fig. 6. The residues after opening the image with increasing structuring element (a disk starting with radius 5).

From the pattern spectrum we can extract different parameters [5], [6] such as:

- *mean object size* (area):

$$S(A; B) = \frac{\sum_n n PS(A; B)(n)}{\sum_{a \in A} A(a)}; \quad (8)$$

- *entropy* (average roughness): a quantification of the shape-size complexity:

$$E(A; B) = - \frac{\sum_n PS(A; B)(n) \log_2 \frac{PS(A; B)(n)}{\sum_{a \in A} A(a)}}{\sum_{a \in A} A(a)}; \quad (9)$$

- *normalised average roughness*:

$$EN(A; B) = \frac{E(A; B)}{\log_2(N + 1)}; \quad (10)$$

- *B-shapiness*: a quantitative measure of the resemblance of the objects to the strel shape:

$$BS(A; B) = \frac{PS(A; B)(N_{max})}{\sum_{a \in A} A(a)}; \quad (11)$$

- *maximal n* (N_{max}): the last bin (the highest n -value, when all image objects are sieved out) of the pattern spectrum histogram.

These parameters provide statistical information about the content of the image, like mean object size, shape, direction, variation, Notice that using a different strel results in another pattern spectrum, and thus in other values for the parameters. In the experiments we will use a square structuring element, in order to be able to compare with the pseudo-granulometry (section III-C).

Since the calculation time of the pattern spectrum is very high, there is need for other, similar techniques [7], [8]. We will investigate two techniques: a *block based technique* and the *pseudo-granulometry by minima of linear openings* [7].

B.2 Block based technique

The block based technique divides the images into smaller blocks that are processed independently. This should lower the total calculation time, but introduces a potential problem: a particle at a block boundary will be treated as multiple particles or as a smaller particle. Or in some cases even as a bigger particle. We investigate the resulting deteriorations experimentally. Different sizes for the subimages are used and verified.

C. Opening tree

The *opening tree* [9] makes it possible to approximate the pattern spectrum for grayscale images, with the calculation time about three orders of magnitude faster than the traditional pattern spectrum calculation. The opening tree is a hierarchical technique where the image pixels are the *leaves* and the *nodes* are made of pairs (h, n) , where h is a grayscale value and n is an opening size. The algorithm works row-per-row or column-per-column, but can be extended to a two dimensional version. In that case we get the so-called *pseudo-granulometry by minima of linear openings* or the *granulometry by maxima of linear openings*. The pseudo-granulometric curve should be a good approximation of a square granulometry because of similar image features. We will test this. For a discussion of the algorithm we refer to the original articles [7], [9].

In the 1D-case we will calculate the horizontal (1d.h), vertical (1d.v) and diagonal (both upper-left to lower-right (1d.dm) and upper-right to lower-left (1d.dp)) opening trees. In the 2D-case we will determine the (pseudo-)granulometry for a horizontal and vertical opening tree (*.hv), for the two diagonal opening trees (*.dd), and for the horizontal, vertical and diagonal opening trees (*.all). We will make a calculation with the maximal openings (max.*) and with the minimal openings (min.*).

The opening tree and pattern spectrum algorithms are written in C.

IV. RESULTS

A. Calculation time

In this section we compare the calculation times for the different algorithms used. Seventeen images with resolution 1300×1030 were processed. The methods are the Fast Fourier Transform histogram, the pattern spectrum algorithm, the pattern spectrum for images divided in subimages, where each subimage is processed independently (split into (3×4) , (10×10) and (20×20) different images), and the opening tree algorithm (1D and 2D).

The average results for one image are: the FFTh algorithm only takes a few seconds, for the opening tree tens of seconds are needed, the calculation time for the block based technique goes from a few hours (20×20 subimages) to a few days (3×4 subimages), while the calculation of the classical pattern spectrum takes a few days.

The calculations were made on a PC with an AMD Athlon XP processor (CPU-speed about 1.6 GHz) and with 1 GB of RAM. Other processes were running on the computers at the same time, though.

For the block based technique, the calculation time is the sum of the different block images. We have not taken into account the time necessary to split the images and merge the results.

The fastest technique is definitely the FFTh, followed by the opening tree algorithm. This algorithm is faster than the exact pattern spectrum algorithm by a factor 2000. This is a remarkable improvement which doesn't seem plausible, but another author [9] also reports time reductions of several orders of magnitude. Note that both algorithms were implemented in C, so the large difference is not due to a big difference in implementation efficiency. The calculation time of $PS(A; B)(n)$ increases (in a nonlinear way) with n , because for every increase of n with 1 an extra erosion and dilatation have to be performed. It is not possible to use previously obtained information from the morphological opening for a calculation with another

n -value. This problem is not present in the opening tree algorithm. The 1D opening tree is five times faster than the 2D opening tree. With the block based technique, the classical algorithm becomes faster (factor 40 when the image has been divided in 400 subimages), but the time necessary to split and merge the (sub)images still has to be taken into account. In section IV-D we will investigate the usefulness of this technique.

B. Fourier Analysis

We calculated six parameters. Table I shows the correlation coefficients P between the different spectrum parameters and the different experimental parameters (frequency, load and temperature). It also shows the value \tilde{P} , the probability of getting a correlation as large as the observed value by random chance, when the true correlation is zero. So it is important that the value for P is close to 1 and the value for \tilde{P} is low. Since there are too few pictures available to do the statistical analysis, the \tilde{P} value will be quite large in most of the reported results. We hope this problem is solved in the future. In the case of the correlation of the temperature with the spectrum parameters no value of \tilde{P} is listed, since only two observations were available.

From the correlation tables we observe the following trends for the parameters from the FFTh:

- **Frequency** is proportional to *entropy*;
- **Temperature** is proportional to *mean* and *standard deviation*;
- **Load** is proportional to *kurtosis* and *skewness* when $T = 100 \text{ }^\circ\text{C}$;
- **Load** is inversely proportional to *energy* and *mean* when $T = 180 \text{ }^\circ\text{C}$;
- **Load** is proportional to *entropy* in both cases but with lesser probability.

Overall, *entropy* correlates best with the physical parameters.

C. Pattern spectrum

The pattern spectrum gives us information about the sizes and shapes of the objects in the image. We calculated the spectrum by using a square structuring element, starting at size 2×2 . Here we calculated five parameters. Table II shows the correlation coefficients P for the different spectrum parameters with the different experimental parameters (frequency, load and temperature).

Some correlation between the parameters from the experiment (frequency, temperature and load) and the parameters from the pattern spectrum can be seen:

- **Frequency** is inversely proportional to *roughness*, *normalised roughness* and *shapiness*;

TABLE I
CORRELATION COEFFICIENTS FOR THE FFTH PARAMETERS

		Mean	Std	Skewness	Kurtosis	Energy	Entropy
Frequency free T, L = 100 N	P	0.60	0.37	-0.64	-0.61	-0.51	0.78
	\tilde{P}	0.59	0.76	0.55	0.59	0.66	0.43
Temperature L = 50 N	P	1	1	1	1	1	-1
	\tilde{P}	—	—	—	—	—	—
Temperature L = 100 N	P	1	1	-1	-1	-1	1
	\tilde{P}	—	—	—	—	—	—
Temperature L = 150 N	P	1	1	1	1	-1	1
	\tilde{P}	—	—	—	—	—	—
Load T = 100 °C	P	-0.14	0.62	0.87	0.86	-0.0087	-0.67
	\tilde{P}	0.86	0.38	0.14	0.14	0.99	0.33
Load T = 180 °C	P	-0.83	-0.25	0.44	0.41	-0.94	-0.63
	\tilde{P}	0.38	0.84	0.71	0.73	0.23	0.57

TABLE II
CORRELATION COEFFICIENTS FOR THE PS PARAMETERS

		Size	Roughness	Norm. roughness	N_{max}	Shapiness
Frequency free T, L = 100 N	P	-0.68	-0.88	-0.94	-0.10	-0.90
	\tilde{P}	0.53	0.32	0.23	0.94	0.28
Temperature L = 50 N	P	-1	1	1	-1	-1
	\tilde{P}	—	—	—	—	—
Temperature L = 100 N	P	-1	-1	1	-1	-1
	\tilde{P}	—	—	—	—	—
Temperature L = 150 N	P	-1	-1	-1	-1	1
	\tilde{P}	—	—	—	—	—
Load T = 100 °C	P	0.55	0.96	0.93	0.88	-0.79
	\tilde{P}	0.45	0.037	0.074	0.12	0.21
Load T = 180 °C	P	0.98	0.95	0.48	0.93	0.51
	\tilde{P}	0.14	0.20	0.68	0.23	0.66

- **Temperature** inversely proportional to *size* and N_{max} ;
- **Load** is proportional to *normalised roughness* when T = 100 °C;
- **Load** is proportional to *size* when T = 180 °C;
- **Load** is proportional to *roughness* and N_{max} in both cases.

Overall, *roughness* and *normalised roughness* correlate best with the physical parameters, and they show the same behaviour.

Compared to the FFTh parameters (section IV-B), there is a better correlation between the experimental parameters and those from the pattern spectrum.

As stated before, the number of pictures that were available is small. Therefore the presented results are preliminary. More data are needed.

D. Block based technique

When the number of subimages increases, the values of *size*, N_{max} and *roughness* decrease. The values of *shapiness* and *normalised roughness* increase. Fig. 7 shows the differences between the pattern spectra. At lower n -values, the spectra from the images divided into more blocks show higher PS-values, but lower PS-values at higher n and lower N_{max} -values. Notice from the insert in fig. 7 that N_{max} for the 3×4-case is higher than the one for the original image. This is due to boundary effects.

If we compare the correlation coefficients P and the coefficients \tilde{P} for the full image (section IV-C) with the in subimages divided images, then we notice the following: when the number of subimages increases the correlation between the frequency and the spectrum parameters im-

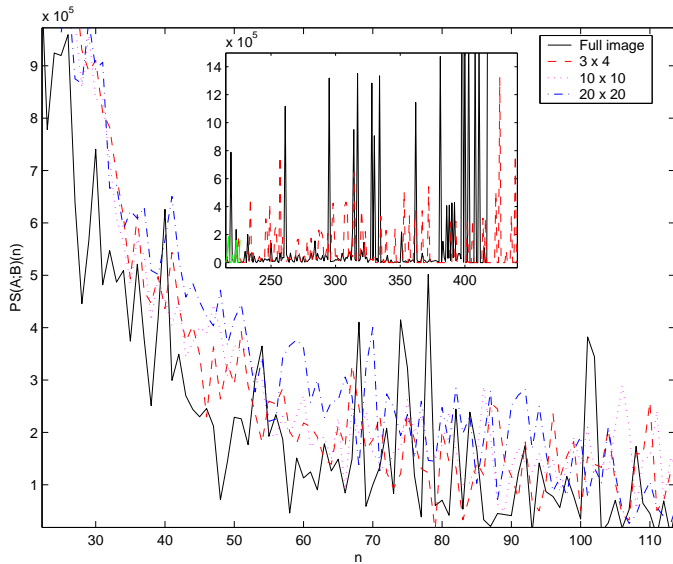


Fig. 7. Part of the Pattern spectrum of the original image and the into subimages divided (and afterwards merged) images.

proves, but it worsens between the load and the spectrum parameters. Also, the parameter N_{max} tends to become inversely proportional with the load.

E. Opening tree

If we compare the pattern spectrum with the 2D opening trees, then we get the following results (fig. 8): `min.all` and `min.dd` visually look more like the exact PS than `min.hv`, but this one is better than the 1D opening trees and `max.all` is the most different. But overall `min.hv`'s parameters agree more with the pattern spectrum than the other opening trees, although values can differ strongly. *Roughness* and *normalised roughness* from `min.hv` agree most with the value from the PS (over 90 % resemblance), followed by the parameter *size* (about 30 % too large). The other parameters differ very much.

Table III shows the correlation coefficients P for the different spectrum parameters of `min.hv` with the different experimental parameters (frequency, load and temperature).

Notice how for N_{max} there is no correlation coefficient available. This is due to the fact that the opening tree algorithm on the present images almost always produces the same value for N_{max} . Therefore no correlation can be found.

Some correlation between the parameters from the experiment (frequency, temperature and load) and the parameters from the opening tree `min.hv` can be seen:

- **Frequency** is inversely proportional to *roughness*, *normalised roughness* and *size*;
- **Temperature** is inversely proportional to *size*;

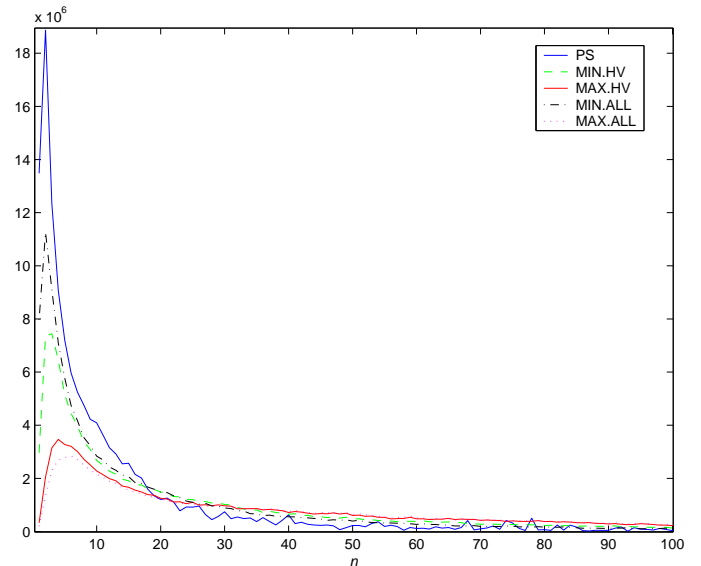


Fig. 8. Comparison of the exact pattern spectrum with some 2D opening trees.

- **Load** is proportional to *roughness* and *normalised roughness* when $T = 100$ °C;
- **Load** is proportional to *shapiness* when $T = 180$ °C;
- **Load** is proportional to *size* in both cases.

Overall, *roughness* and *normalised roughness*, which show almost exactly the same correlation, and *size* correlate best with the physical parameters.

For the other types of opening trees similar results are obtained. There are slight differences between the diagonal opening trees and the other trees, but they are not significant.

It seems that the parameters from the PS (section IV-C) are better correlated with the experimental parameters than the parameters from the opening tree are.

V. CONCLUSIONS

Although the images don't contain enough debris particles and there are too little number of pictures to draw definite and reliable conclusions, some indications for correlation between the parameters of the FFTh/PS/opening tree and the physical parameters from the experiment can be seen.

The Fast Fourier Transform histogram is a fast technique where the parameter *entropy* is the best to classify the differently threated images. For the pattern spectrum algorithm the parameters *roughness* and *normalised roughness* are the best, but this technique is very slow. The opening tree algorithm is very fast compared to the exact pattern spectrum algorithm and gives similar results (especially `min.hv`). *Size* is a useful parameter.

Concluding from the obtained results, the opening tree

TABLE III
CORRELATION COEFFICIENTS FOR THE MIN.HV PARAMETERS

		Size	Roughness	Norm. roughness	N_{max}	Shapiness
Frequency free T, L = 100 N	P	-0.77	-0.85	-0.85	—	-0.54
	\tilde{P}	0.44	0.36	0.36	—	0.64
Temperature L = 50 N	P	-1	1	1	—	1
	\tilde{P}	—	—	—	—	—
Temperature L = 100 N	P	-1	-1	-1	—	1
	\tilde{P}	—	—	—	—	—
Temperature L = 150 N	P	-1	1	1	—	-1
	\tilde{P}	—	—	—	—	—
Load T = 100 °C	P	0.88	0.90	0.90	—	0.23
	\tilde{P}	0.12	0.097	0.097	—	0.77
Load T = 180 °C	P	0.95	0.60	0.60	—	0.79
	\tilde{P}	0.20	0.59	0.59	—	0.42

is preferred to the FFTh because of its correlation accuracy and to the PS because its huge speed improvement.

VI. FUTURE WORK

In the future we analyse more images with more debris particles present. We will also do something about the speckled background of the pictures (fig. 2).

If the colour content could be incorporated in the algorithms, it would give us extra information.

REFERENCES

- [1] J. Halling. *Principles of Tribology*. Macmillan Publishing Ltd, 1973.
- [2] S. Huguet, N. Godin, R. Gaertner, L. Salmon, and D. Villard. Use of Acoustic Emission to Identify Damage Modes in Glass Fibre Reinforced Polyester. *Composites Science and Technology*, 62(10–11):1433–1444, 2002.
- [3] W.K. Pratt. *Digital Image Processing*. John Wiley & Sons, 3rd edition, 2001.
- [4] R.M. Haralick and L.G. Shapiro. *Computer and Robot Vision*, volume 1, chapter 5. Addison-Wesley, 1992.
- [5] P. Maragos. Pattern Spectrum and Multiscale Shape Representation. *IEEE Transactions on Pattern Analysis and Machine Intelligence*, 11(7):701–716, 1989.
- [6] S. Banerjee and S.C. Sahasrabudhe. C-factor: a morphological shape descriptor. *Journal of Mathematical Imaging and Vision*, 4:43–55, 1994.
- [7] L. Vincent. Granulometries and Opening Trees. *Fundamenta Informaticae*, 41(1–2):57–90, 2000.
- [8] A. Meijster and M.H.F. Wilkinson. A Comparison of Algorithms for Connected Set Openings and Closings. *IEEE Transactions on Pattern Analysis and Machine Intelligence*, 24(4):484–494, 2002.
- [9] L. Vincent. Fast Grayscale Granulometry Algorithms. In *Proceedings of ISMM'94 International Symposium on Mathematical Morphology*, pages 265–272, Fontainebleau, France, 1994.